The recruitment of p47phox and Rac2G12V at the phagosome is transient and phosphatidylserine-dependent

Marie-Cécile Faure, Jean-Claude Sulpice, Maud Delattre, Marc Lavielle, Magali Prigent, Marie-Hélène Cuif, Chantal Melchiort, Eric Tschirhart, Oliver Nusse, Sophie Dupre-Crochet

The recruitment of p47^{phox} and Rac2G12V at the phagosome is transient and phosphatidylserine-dependent

Marie Cécile Faure*[†‡], Jean-Claude Sulpice[†], Maud Delattre*[§], Marc Lavielle*[§], Magali Prigent*[‖], Marie-Hélène Cuif*[‖], Chantal Melchior[‡], Eric Tschirhart[‡], Oliver Nüβe*[†] and Sophie Dupré-Crochet*[†]

* Univ. Paris-Sud, Orsay F-91405, France
† INSERM UMRS757, Orsay F-91405, France
‡ Life Sciences Research Unit, University of Luxembourg, Luxembourg L-1511, Luxembourg
§ INRIA Saclay Ile-de-France, Orsay F-91893, France
‖ CNRS UMR8621, Institut de Génétique et Microbiologie, Orsay F-91405, France

Running title: PS and phagosomal accumulation of p47^{phox} and Rac2

Corresponding author:
Sophie Dupré-Crochet
Univ Paris-Sud, INSERM U757, Bldg 443, 15 R Georges Clemenceau, F-91405 Orsay, France; phone: ++33 (0)169156861; fax: ++33 (0)169155893;
e-mail: sophie.dupre@u-psud.fr

Key words :
ROS production, live imaging, anionic phospholipids, NADPH oxidase, phagocytosis

Abbreviations: $DCFH_2$**,** 2', 7'-dichlorodihydrofluorescein diacetate, succinimidyl ester**;** lactC2, C2 domain of lactadherin; $O_2^{\bullet-}$, superoxide anion; PLB-985 cells, myeloid leukemia cell line; PA, phosphatidic acid; (PI(3)P), phosphatidylinositol-3-phosphate PI(3,4)P2, phosphatidylinositol (3,4)bisphosphate; PPI, phosphoinositides; PS, phosphatidylserine; PX domain, phox homology domain; ROS, reactive oxygen species.

Graphical abstract: Phagocytes produce ROS via the NADPH oxidase to kill pathogens in the phagosome. The activation of the NADPH oxidase depends on the translocation of cytosolic subunits (p40^{phox}, p47^{phox}, p67^{phox}) and Rac2 to the membrane subunits (gp91^{phox} and p22^{phox}).
Our data indicate that p47^{phox} and Rac2 only briefly translocate to the phagosome while ROS production continues for a longer period. Furthermore, phosphatidylserine appears as a modulator of subunit recruitment and ROS production.

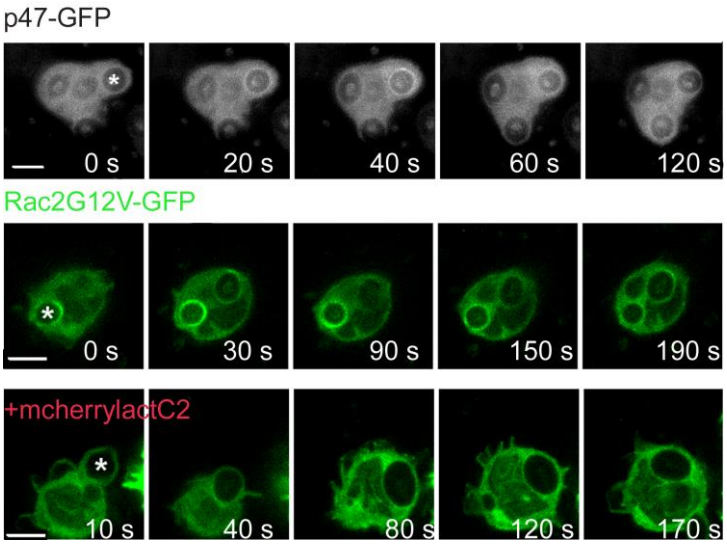

Abstract

Background information: During phagocytosis, neutrophils internalize pathogens in a phagosome and produce reactive oxygen species (ROS) by the NADPH oxidase to kill the pathogen. The cytosolic NADPH oxidase subunits $p40^{phox}$, $p47^{phox}$, $p67^{phox}$ and Rac2 translocate to the phagosomal membrane to participate in enzyme activation. The kinetics of this recruitment and the underlying signalling pathways are only partially understood. Anionic phospholipids, phosphatidylserine (PS) and phosphoinositides (PPI) provide important attachment site for numerous proteins, including several oxidase subunits.

Results: We investigated the kinetics of $p47^{phox}$ and Rac2 phagosomal membrane recruitment. Both subunits are known to interact with anionic phospholipids; we therefore addressed the role of PS in this recruitment. Phagosomal accumulation of $p47^{phox}$ and Rac2 tagged with fluorescent proteins was analyzed by videomicroscopy. We used the C2 domain of lactadherin (lactC2) that interacts strongly and specifically with PS to monitor intracellular PS localization and to decrease PS accessibility. During phagocytosis of opsonized zymosan, $p47^{phox}$ and constitutively active Rac2G12V briefly translocated to the phagosomal membrane while ROS production continued for a longer period. However, in the presence of lactC2, Rac2G12V recruitment was inhibited and the kinetics of $p47^{phox}$ recruitment and detachment were delayed. A reduced phagosomal ROS production was also observed during the first seven minutes following the phagosome closure.

Conclusions: These results suggest that $p47^{phox}$ and Rac2 accumulate only transiently at the phagosome at the onset of NADPH activity and detach from the phagosome before the end of ROS production. Furthermore, lactC2, by masking PS, interfered with the phagosomal recruitment of $p47^{phox}$ and Rac2 and disturbed NADPH oxidase activity. Thus, PS appears as a modulator of NADPH oxidase activation.

Introduction

During bacterial and fungal infections, phagocytes play a major role in host defence. Neutrophils are the first cells that arrive at the site of infection, ingest the pathogen into a compartment called phagosome and kill it inside this phagosome. Phagocytes express the enzyme NADPH oxidase that generates superoxide anion ($O_2^{\bullet-}$) by transferring electrons from NADPH to molecular oxygen. $O_2^{\bullet-}$ and the other derivative reactive oxygen species (ROS) produced in the phagosome, participate in the killing of the pathogenic agent. Genetic deficits in NADPH oxidase lead to chronic granulomatous disease (CGD) characterized by severe recurrent infections (Stasia and Li, 2008). NADPH oxidase is a multicomponent enzyme composed of membrane associated proteins, $gp91^{phox}$ and $p22^{phox}$, cytosolic proteins, $p67^{phox}$, $p47^{phox}$, $p40^{phox}$ and the small G protein Rac. Upon stimulation via soluble or particulate stimuli, the cytosolic subunits translocate to the plasma or phagosomal membrane and assemble with the membrane subunits to form an active enzyme (Nauseef, 2004). This translocation induces the activation of the NADPH oxidase. In the resting state, the three cytosolic subunits, $p67^{phox}$, $p47^{phox}$, $p40^{phox}$ form a heterotrimeric complex in the cytosol (Groemping and Rittinger, 2005). It is unclear, whether these subunits translocate together or sequentially and whether they remain together to form the active enzyme for the entire time of ROS production.

Upon stimulation, $p47^{phox}$ attaches to the membrane via its PX domain and to $p22^{phox}$ via its SH3 domains and thereby translocates the complex to the membrane (Kanai et al., 2001; Ago et al., 2003; Groemping and Rittinger, 2005). Rac1 and Rac2 are involved in phagocytosis and $O_2^{\bullet-}$ generation (Quinn et al., 1993; Caron and Hall, 1998; Mizrahi et al., 2010) . However they may have different roles and it has been proposed that Rac2 is more specific for ROS production (Filippi et al., 2004). It has been shown in vitro that phospholipids and especially phosphatidylserine (PS) are essential for oxidase activation (Tamura et al., 1988; Shpungin et al., 1989) . The translocation of Rac, $p47^{phox}$ and $p40^{phox}$ to the membrane involve direct interaction with anionic lipids mainly PPI, phosphatidic acid (PA) and PS. In fact, $p47^{phox}$ and $p40^{phox}$ bear a lipid binding domain: the phox homology (PX) domain. The PX domain of $p47^{phox}$ has two binding pockets: one preferentially binds to phosphatidylinositol-(3,4)-bisphosphate ($PI(3,4)P_2$) and the other binds to PA and PS whereas the PX domain of $p40^{phox}$ binds to phosphatidylinositol-3-phosphate (PI(3)P) (Kanai et al., 2001; Karathanassis et al., 2002). The role of the PX domain in $p47^{phox}$ may depend on the type of stimulation. The disruption of PI(3,4)P2 binding in this domain does not prevent phagosomal translocation (Li et al., 2010). Rac proteins, like many other small GTPases, contain a polybasic domain (Williams, 2003) that has been shown to act as a targeting signal to localize proteins to membranes (McLaughlin and Aderem, 1995; Yeung et al., 2006; Yeung et al., 2008). The negative charge of the cytosolic leaflet of cellular membranes depends on their anionic phospholipid content. It creates an electrostatic field that attracts proteins with cationic residues such as the small GTPases (Yeung and Grinstein, 2007). Using cationic probes (Roy et al., 2000), Yeung et al. showed that the surface charge of the cytosolic leaflet of the phagosome decreased during phagocytosis (Yeung et al., 2006; Yeung et al., 2009). This decrease was attributed mainly to the drop in phosphatidylinositol-(4,5)-bisphosphate that occurred upon closure of the phagosome (Botelho et al., 2000; Steinberg and Grinstein, 2008) . PS, which represents about 15% of the lipids in the inner leaflet of the plasma membrane (Yeung and Grinstein, 2007), persists on the phagosome after sealing and contributes to the phagosomal surface charge (Yeung et al., 2009; Magalhaes and Glogauer, 2010; Minakami et al., 2010) . In the previous studies, the phagosomal PS content

was monitored using the C2 domain of the lactadherin fused to a fluorescent protein as a probe. The lactadherin and its C2 domain (lactC2) were shown to bind phosphatidylserine specifically and with a high affinity (Kd around 2 nM for both), in a calcium independent manner (Andersen et al., 2000; Shi et al., 2004). By contributing to the phagosomal surface charge as well as binding to specific protein domains, PS could play a role in NADPH oxidase activation. Rac and $p47^{phox}$ are good candidates for a PS dependent recruitment to the membrane as explained above.
In this study, we investigated the kinetics of Rac and $p47^{phox}$ recruitment at the phagosome and the role of PS in their recruitment. To examine this latter point we used the lactC2 probe. Indeed, *in vitro* studies demonstrated that lactadherin inhibits enzyme complexes of blood coagulation by blocking PS binding sites (Shi and Gilbert, 2003). We then reasoned that lactC2 may have a dual role in the cell serving as a probe to monitor PS but also masking PS. We observed that $p47^{phox}$ and a dominant positive form of GFP-Rac2 (GFP-Rac2G12V) were transiently recruited at the phagosomal membrane, at the beginning of phagocytosis and left the phagosome far before the termination of ROS production. In the presence of mCherry-lactC2 the phagosomal recruitment of GFP-Rac2G12V was blocked and p47-GFP translocation slowed down. We then looked at NADPH oxidase activity in cells expressing mcherry-lactC2. The phagosomal ROS production was reduced at the commencement of phagocytosis. These results advocate that lactC2, by masking PS, interfered with the phagosomal recruitment of $p47^{phox}$ and Rac2 and disturbed NADPH oxidase activity.

Results

Generation of stable PLB-985 cell lines expressing p47-GFP and CFP-Rac2

To examine the accumulation of p47phox and Rac2 at the phagososome we generated neutrophil-like cells (differenciated myeloid leukemia cell line, PLB-985 cells) with stable expression of p47-GFP and CFP-Rac2. The level of transgenic protein expression was assessed by flow cytometry (data not shown) and by immunoblot analysis (Fig. 1A). The immunot blot with anti-GFP reveals that only the tagged proteins are expressed in the cells and not the GFP alone. The immunoblot with anti-$p47^{phox}$ shows that the level of endogenous $p47^{phox}$ was 5 fold higher than the p47-GFP level in the p47-GFP transgenic cell line (Fig. 1B). In the CFP-Rac2 transgenic cell line similar level of CFP-Rac2 and endogenous Rac2 were observed (Fig. 1C). We further measured the ROS production in the two transgenic cells lines in response to phorbol 12-myristate acetate (PMA) by using a luminol assay. ROS production of both lines was similar to non-transfected differentiated cells (data not shown). Immunoprecipitation experiments were then performed to check the interactions of p47-GFP and CFP-Rac2 with the other endogenous NADPH oxidase subunits. Both transgenic PLB-985 cell lines were stimulated by PMA for 10 min and the oxidase membrane subunit $gp91^{phox}$ was immunoprecipitated from the membrane fraction. As shown in Figure 1D, $gp91^{phox}$ co-immunoprecipitated with p47-GFP as well as endogenous $p47^{phox}$ and $p67^{phox}$ in the p47-GFP transgenic PLB-985 cell line. The same result was obtained with CFP-Rac2 in the transgenic CFP-Rac2 PLB-985 cell line (Fig. 1E). In the control, agarose beads alone without $gp91^{phox}$ antibodies collected tenfold less $gp91^{phox}$ than with the specific $gp91^{phox}$ antibodies.

P47^{phox} is transiently recruited to the phagosome

The recruitment of p47-GFP was then followed during phagocytosis of opsonized zymosan by wide field videomicroscopy. The cytosolic marker calcein blue was measured in the same cells in order to quantify p47-GFP fluorescence by ratio analysis. The mean time from phagosomal cup formation to phagosome closure, was 48 +/- 5 s (n=12). Accumulation of P47-GFP was first visible at the phagosomal cup on average 14 +/- 5 s (n=14) before sealing (Fig. 2B). Then p47-GFP fluorescence increased rapidly at the phagosome, with a maximal fluorescence 20s after the phagosome closure, and then decreased (Fig. 2A, C and video S1). Quantification of p47-GFP phagosomal recruitment was performed by measuring the ratio of phagosomal to cytosolic fluorescence. P47-GFP was present at the phagosomal membrane for only 2 min after the phagosome closure (Fig. 2C). To confirm that p47-GFP reflected the properties of endogenous p47^{phox}, we performed immunofluorescence experiments using a protocol of synchronized phagocytosis (Quinn et al., 2007). Cells were incubated with opsonized texas-red zymosan (time 0); then the number of phagosomes and the presence of phagosomal p47^{phox} were determined at different time points after incubation. Most of the phagocytosis occurred during the first five minutes (Fig. 2E). In these conditions, we observed a decrease in p47^{phox} positive phagosomes from 50% to 25% during the first five minutes and then p47^{phox} presence diminished to 11% after 10 minutes (Fig. 2D, E). The remaining p47^{phox} positive phagosomes at 10 min were most likely formed during the preceding 5 min. This result confirms that endogenous p47^{phox}, like p47-GFP, is transiently recruited at the phagosome and leaves the phagosome within a few minutes.

The accumulation of Rac2G12V at the phagosome is also transient

We next investigated the CFP-Rac2 translocation at the phagosome during zymosan phagocytosis by videomicroscopy. However, we could not observe any consistent accumulation of CFP-Rac2 at the phagosome (data not shown). The same result was obtained with PLB-985 cells stably expressing GFP-Rac2 (data not shown). This may be due to abundant endogenous Rac2 which might compete with CFP-Rac2 (or GFP-Rac2) for activation and phagosomal membrane targeting. Therefore, we used the constitutively active form Rac2G12V which displaced the equilibrium Rac2GDP/Rac2GTP in favor of the GTP bound Rac2G12V form. Differentiated PLB-985 cells were transiently transfected with GFP-Rac2G12V and the fusion protein was followed during phagocytosis of zymosan by spinning-disk confocal videomicroscopy (Fig. 3A, video S2). In these cells expressing GFP-Rac2G12V, the formation of the phagosome, from the visible cup until phagosome sealing, lasted 48 s +/- 5 s (mean +/-SD, n=9) and GFP-Rac2G12V was first visible at the cup 15 s +/- 6 s (mean +/-SD, n=11) prior to phagosome closure (Fig. 3B). As for p47-GFP, the GFP-Rac2G12V fluorescence increased rapidly at the phagosome, with a maximal fluorescence 20 s after the phagosome closure, and then decreased (Fig. 3A, C and video S2). The fluorescence ratio between phagosome and cytosol was calculated to evaluate the protein accumulation at the phagosome. The mean time of GFP-Rac2G12V accumulation at the phagosomal membrane was 3 min (Fig. 3C).

Phosphatidylserine is localized at the phagosomal membrane and its presence decreases slowly after the phagosomal closure

As the accumulation of p47 and Rac2G12V at the phagosome may require attachment to anionic phospholipids, we wanted to investigate the role of PS in this process. We first monitored PS accumulation at the phagosome of PLB-985 cells during phagocytosis with the C2 domain of lactadherin that binds specifically to PS (lactC2). The lactC2 domain was fused to the fluorescent protein mCherry, this fusion protein was transiently transfected into differentiated PLB-985 cells,

and the distribution of the mCherry-lactC2 probe was visualized during yeast phagocytosis by 3D deconvolution microscopy. At time 0, when the phagosome closed, the lactC2 probe marked the inner leaflet of the plasma membrane as well as the cytosolic leaflet of the phagosomal membrane (Fig.4A), as observed by Minakami et al. in human neutrophils (Minakami et al., 2010). We also witnessed a cytosolic fluorescence due to the presence of free probe in the cytosol. Following yeast internalization, the lactC2 fluorescence at the phagosome decreased slowly. Quantification of mcherry-lactC2 phagosomal accumulation was performed by measuring the ratio of phagosomal to cytosolic fluorescence. As shown in Figure 4B, the fluorescence ratio decreased from 1.61 at time 0 to 1.26 within 20 min. Statistical analysis shows that this ratio was significantly reduced 15 and 20 min after the phagosome closure, revealing a slow decrease of the phosphatidylserine content in the cytosolic leaflet of the phagosomal membrane. These results indicate that, in PLB-985 cells, the phagosomal accumulation of PS was slowly reduced to reach nearly 50% reduction 20 min after the phagosome closure.

LactC2 expression disturbs p47-GFP accumulation at the phagosome

As the phagosome was enriched in the lactC2 probe especially during the first 20 min after closure, lactC2 could mask phagosomal PS similar to the effects seen with whole lactadherin (Hanayama et al., 2002; Shi and Gilbert, 2003; Asano et al., 2004). Therefore lactC2 may interfere with $p47^{phox}$ and Rac2 phagosomal membrane targeting. The effect of the lactC2 probe on $p47^{phox}$ phagosomal recruitment was assessed by transiently transfecting the stable cell line p47-GFP with mCherry-lactC2. Then the accumulation of p47-GFP at the phagosome during phagocytosis of opsonized zymosan was monitored by wide field videomicroscopy as before. P47-GFP was still recruited in the cells that expressed mCherry-lactC2 as revealed by the p47-GFP fluorescent ring around the phagosome (Fig. 5A). However the kinetics of p47-GFP accumulation was modified in these cells compared to control cells. In mCherry-lactC2 co-expressing cells $p47^{phox}$ -GFP was still present at the phagosomal membrane 240 s after the phagosome closure whereas it had already disappeared at 120 s in cells that did not express the mCherry-lactC2 probe (Fig. 5B). To highlight the impact of lactC2 on p47-GFP translocation, the phagosomal recruitment of p47-GFP was modeled after a monocompartmental pharmacokinetics equation (see materials and methods section for detailed explanation of the method). Comparison of the constant of recruitment k2 between the two cell populations indicates that the recruitment of p47-GFP was significantly decelerated in cells expressing the lactC2 probe compared to control cells: k2 = 2.1 min^{-1} for control cells and 1.0 min^{-1} for lactC2 expressing cells (statistical Wald test, p = 0.029). Interestingly, the detachment of p47-GFP was also hindered in lactC2 expressing cells, as revealed by the diminution of the constant of detachment k1: 0.4 min^{-1} for control cells and 0.2 min^{-1} in lactC2 cells (statistical Wald test, p = 0.004). Thus, the lactC2 probe interfered with p47-GFP phagosomal accumulation. This is further illustrated by the increase in time needed to reach the maximal phagosomal recruitment of p47-GFP, Tmax, which was 0.6 min in control cells and 1.4 min in lactC2 expressing cells. However the maximal quantity of p47-GFP recruited at the phagosome (Rmax) appeared unaffected. Actually Rmax was 1.15 in control cells and 1.13 in lactC2 cells. These results indicate that the presence of the lactC2 probe results in a delay of p47-GFP dynamics.

LactC2 expression prevents Rac2 but not Rac1 accumulation at the phagosome

As the surface charge of membrane cytosolic leaflet is important of Rac recruitment (McLaughlin and Aderem, 1995; Yeung et al., 2006; Yeung et al., 2008), the presence of lactC2 at the phagosomal membrane may disturb its recruitment. To investigate the effect of lactC2 expression

on GFP-Rac2G12V translocation to the phagosomal membrane, mCherry-lactC2 and GFP-Rac2G12V were transiently co-expressed in the cells. GFP-Rac2G12V accumulation at the phagosome was then monitored during phagocytosis of opsonized zymosan by spinning disk confocal microscopy. In the presence of mCherry-lactC2, GFP-Rac2G12V was no more recruited at the phagosomal membrane (Fig. 5C and video S3). The fluorescence ratio of phagosome against cytosol was lower than one, emphasizing the absence of GFP-Rac2G12V recruitment in mCherry-lactC2 expressing cells (Figure 5D). As Rac 2 is no more recruited at the phagosome in the presence of the lactC2 probe we wondered whether this was also the case for Rac1. We repeated the same experiment with GFP-Rac1G12V. As previously described (Magalhaes and Glogauer, 2010), GFP-Rac1G12V was present at the plasma membrane and decreased from the phagosome after sealing (Fig. 6A, C). In some videos, however, we could observe a very brief increase of the phagosomal fluorescence after the phagosome closure (Fig. 6A). A similar phenomenon was observed in the cells expressing mcherry-lactC2 (Fig. 6B, C and video S4). In both cases, Rac1G12V was present at the phagosome for at least 10 min (Fig. 6C). Thus Rac1G12V is present on the phagosome from the beginning and its presence is not affected by lactC2.

Binding of the lactC2 probe on phosphatidylserine induces a delay in the ROS production

As the recruitment of p47-GFP and GFP-Rac2G12V was modified, we wondered if the lactC2 probe could have an effect in ROS production. We have previously shown that $DCFH_2$-yeast is a valuable tool to measure ROS production inside the phagosome by video-microscopy until 30 minutes (Tlili et al., 2012) with no photooxydation (Tlili et al., 2011). We could not use $DCFH_2$-zymosan because due to its small size less DCFH2 is attached to the zymosan as compared to yeast and the saturation of the probe in the phagosome is reached after five minutes of ROS production (unpublished observations). Thus the effect of the lactC2 probe on the amplitude and kinetics of the ROS production was assessed with $DCFH_2$-yeast by videomicroscopy. Phagocytosis of $DCFH_2$-yeasts was filmed and the measure of the yeast fluorescence allowed quantifying cellular ROS production inside the phagosome (Fig. 7A,B). During the first minutes after the phagosome closure, the oxidative burst was reduced in mCherry-lactC2 expressing cells compared to mCherry control cells. This initial delay that occurred during the first 7 min following the phagosome closure was compensated at 10 min (Fig 7C). To analyze more precisely the kinetics of the ROS production in the two cell populations, expressing or not the mCherry-lactC2 probe, we took advantage of the Monolix software that is widely used for pharmacokinetics studies (Lavielle and Mentre, 2007). This approach is based on the non linear mixed effects modeling of data (see materials and methods section for detailed explanation of the method). Because we measured an enzymatic activity, we selected a sigmoid model to describe the kinetics of ROS production. The time course of the median $DCFH_2$-yeast fluorescence is well correlated between the experimental data and the values predicted by the model (Fig. S5). The time needed to reach half of the maximal fluorescence (Tc) for the control mCherry expressing cells and for the mCherry-lactC2 cells is significantly increased in cells that express the lactC2 probe : 6.3 min for mCherry expressing cells and 10.7 min for mCherry-lactC2 cells (statistical Wald test, $p = 0.008$). The initial reaction rate is also decreased more than 2 fold for the mCherry-lactC2 cells expressing cells (31 units/min) as compared to mcherry cells(68 units/min) . These results indicate that the initial ROS production is significantly reduced in lactC2 expressing cells, probably by masking PS on the phagosomal membrane.

Discussion

Our results show that $p47^{phox}$ and a tagged version of the dominant positive form of Rac2 are recruited to the phagosome for only 2-3 min after phagosome sealing. The presence of lactC2 at the phagosome disturbs p47-GFP accumulation and prevents GFP-Rac2G12V recruitment at the phagosome. In PLB-985 cells expressing lactC2 the ROS production is also reduced during the first seven minutes following phagosome sealing.

As previously observed (Ueyama et al., 2008; Li et al., 2010), p47-GFP was recruited at the phagosomal membrane just before phagosome closure and then accumulated at the phagosome. However, we observed that p47-GFP remained accumulated for only 2 min. This was unexpected since we had previously observed a stable association of p67-GFP at the phagosome for 45min under similar conditions of phagocytosis (Tlili et al., 2012). Immunofluorescence experiments confirmed the transient translocation of endogenous $p47^{phox}$ to phagosomes containing opsonized zymosan. Other immunofluorescence studies do not agree with this transient translocation of $p47^{phox}$ however this may depend on the amount of zymosan in the experiment which is a key element for the synchronization of phagocytosis (Allen et al., 1999). We could not detect any reproducible accumulation of wild type CFP-Rac2 or GFP-Rac2 at the phagosomal membrane. A discrete and brief enrichment of tagged Rac2 on the phagosome has been observed in Raw 264.7 cells (Hoppe and Swanson, 2004). The visualisation of a phagosomal localisation of a tagged Rac2 depends on the amount of protein that is recruited and on its time of presence at the phagosome. Our fractionation experiments indicate that less than 5% of the CFP protein is translocated to the plasma membrane upon PMA stimulation (data not shown). The recruitment and the time of presence of Rac2 at the phagosome depend on the regulation of this small GTPase by RhoGDI, GEFs and GAPs and others factors such as the surface charge of the membrane. Rac proteins have a polybasic domain: the Rac2 polybasic domain is moderately charged (+3) whereas the Rac1 domain carries more positive charges (+6). We have shown here that a dominant positive mutant of Rac2, Rac2G12V, is recruited at the phagosomal cup just before sealing whereas the corresponding mutant of Rac1 accumulated at the plasma membrane and started to detach upon phagosome sealing. Similar results were obtained for the other dominant positive mutants Rac1Q61L and Rac2Q61L (Yeung et al., 2006; Magalhaes and Glogauer, 2010). The accumulation of constitutively active Rac2 and the detachment of constitutively active Rac1 correlated with the decrease of the surface charge of the phagosome (Yeung and Grinstein, 2007; Magalhaes and Glogauer, 2010). Thus, the charges in the polybasic domain appeared to be important for the phagosomal accumulation of GTP bound Rac. We showed that Rac2G12V is only accumulated at the phagosome for 3 min after phagosome closure and leaves the phagosome well before termination of ROS production that lasted more than 10 min (Fig. 7C). Magalhaes et al. observed that Rac2Q61L was still at the phagosomal membrane 30 min after particle internalization (Magalhaes and Glogauer, 2010). This difference may be explained by the differential regulation of the two dominant positive mutant proteins. Both mutations inhibit the intrinsic and GAP-stimulated GTP hydrolysis (Xu et al., 1994). However RacG12V, like wild type Rac and contrary to RacQ61L, can interact with GEF and with RhoGDI (Xu et al., 1997; Ugolev et al., 2006). Accordingly, the regulation of Rac2G12V would be closer to that of wild type Rac2. We were unable to identify an anti-Rac2 antibody suitable for immunostaining to examine the translocation of endogenous Rac2.

To monitor PS localization and decrease its accessibility, we used the lactC2 probe that interacts specifically with PS (Yeung et al., 2008). As previously observed (Yeung et al., 2009; Magalhaes and Glogauer, 2010; Minakami et al., 2010), the lactC2 probe marked the cytosolic leaflet of the

phagosome. In the neutrophil-like PLB-985 cells, we observed that lactC2 remained accumulated at the phagosome after particle internalization and that the ratio phagosome/cytosol slowly decreased over 20min. The PS content of the phagosome is probably modulated by PS metabolism and vesicular traffic. The removal of membrane material enriched in PS, from macrophage phagosomes has been described (Yeung et al., 2009). Lactadherin and its C2 domain bind PS with high affinity and selectivity (Andersen et al., 2000; Shi et al., 2004; Shao et al., 2008) and an extracellular mutant of lactadherin could mask PS on the outer leaflet of the plasma membrane (Hanayama et al., 2002; Shi and Gilbert, 2003). Therefore, lactC2 inside the cell could have a dual role serving as a probe to monitor PS but also masking PS. LactC2 masks probably a few percent of the PS, which has an estimated cellular concentration of 100µM (Kay et al., 2012), however a substantial part of the PS may be associated with protein complexes (Kay et al., 2012) and consequently not be accessible to the lactC2 probe and other endogenous proteins. So, the presence of the lactC2 probe decreases the fraction of "accessible PS". Indeed, we could show that the lactC2 probe interferes with cellular functions, it modifies Rac2G12V and p47-GFP recruitment and reduces ROS production during the first seven minutes after the phagosome closure. The reduced PS accessibility could explain these defects.

Our results suggest that lactC2 prevents Rac2 recruitment at the phagosome. Absence of phagosomal Rac2 may explain the reduced initial ROS production. One might expect that the absence of Rac2 leads to a stronger defect. However it has been shown that neutrophils expressing a dominant negative form of Rac2 have only a modest defect in $O2^{\cdot-}$ production in response to opsonized zymosan (Ambruso et al., 2000; Williams et al., 2000). Furthermore, Rac1 is present in our cells. We observed that, in cells expressing or not mcherry-lactC2, GFP-Rac1G12V is present at the phagosome during its formation and then starts to detach from the phagosome after sealing. Thus Rac1 can probably partly support Rac2 function, when Rac2 is absent. Rac1 localization at the plasma membrane is not affected by lactC2 since Rac1 has been shown to interact preferentially with PS (Finkielstein et al., 2006) and may have a better affinity than lactC2 probe for the negative cytosolic leaflet of the plasma membrane due to its larger polybasic domain. .

$P47^{phox}$, via its PX domain, binds PS (Karathanassis et al., 2002; Stahelin et al., 2003). The specific role of PS in the phagosomal translocation of $p47^{phox}$ has not been established. In the presence of mCherry-lactC2 at the phagosome, the recruitment of p47-GFP is slowed down and its time of presence at the phagosome is increased two fold. The mathematical model suggests that attachment as well as removal of $p47^{phox}$ from the phagosome is slowed down. The PX domain alone does not accumulate at the phagosomal membrane ((Johnson et al., 2006) and unpublished data). However, our data suggest that this domain is important for the kinetics of $p47^{phox}$ accumulation at the phagosome: by reducing the accessibility to PS, we slowed down $p47^{phox}$ recruitment. Masking PS with lactC2 may also have indirect effects on the accumulation of p47-GFP at the phagosomal membrane by interfering with other proteins. For example, the phosphorylation of $p47^{phox}$ by PKC may be reduced because the PS binding domain (C2 domain) of PKC isoforms is important for its localization and activation (Conesa-Zamora et al., 2001). The mutant p47R90A, which has a reduced affinity for $PI(3,4)P_2$ but binds to PA and PS, translocated to the phagosomal membrane and restored ROS production of $p47^{phox}$ KO mouse neutrophils (Li et al., 2010). The translocation of this mutant presumably relies on a direct interaction with PA, PS and $p22^{phox}$. Taken together, these observations confirm the concept that membrane translocation of $p47^{phox}$ is based on a multicomponent interaction system (Steinberg and Grinstein, 2008) to insure maximal flexibility. PS would be one of the targeting motifs of this system.

To summarize, we propose the following model (Fig. 8): Rac2 and $p47^{phox}$ would be recruited at the same time at the phagosomal cup just before phagosome sealing (Fig.8A). The surface charge of the phagosome conferred by PPI, PA and PS is important for Rac2 recruitment. The Rac2 protein would serve as an adapter to correctly position $p67^{phox}$ toward $gp91^{phox}$; (Fig.8B) then it detaches from the phagosome a few minutes after sealing (Fig.8C). $P47^{phox}$, via its PX domain binding to PS and $PI(3,4)P_2$ and its SH3 domain binding to $p22^{phox}$, would act as a carrier protein, targeting $p67^{phox}$ and $p40^{phox}$ to the NADPH oxidase complex (Fig.8A,B). Once the complex is assembled $p47^{phox}$ detaches a few minutes after phagosomal closure (Fig.8C). $PI(3,4)P_2$ accumulates at the phagosome during its formation and remains present during the first minute after closure, whereas PI(3)P starts to accumulate 1 min after phagosome sealing (Fig8. B, C).. $P67^{phox}$ would remain assembled with the membrane subunits via its interaction with $gp91^{phox}$ and $p40^{phox}$ that binds to PI(3)P (Fig.8C).
A reduced PS level on the phagosomal membrane should affect the ROS production inside the phagosome and may contribute to intraphagosomal survival of pathogens. Indeed, certain pathogens such as *Listeria pneumophilia* are able to decrease the PS content of the phagosome within a few hours (Yeung et al., 2009).

Materials and methods

Cell culture

The human myeloid leukemia cell line PLB-985 was a generous gift from Marie-José Stasia (Grenoble, France). Cells were cultured as previously described (Tlili et al., 2011). The differentiation towards neutrophil-like cells was induced by addition of 1.25% dimethylsulfoxide (DMSO) to exponentially growing cells for 5 or 6 days. For all experiments, differentiated PLB-985 cells were centrifuged 3 min at 2000 rpm and resuspended in Hepes buffer containing 140 mM NaCl, 5 mM KCl, 1 mM $MgCl_2$, 2 mM $CaCl_2$, 10 mM Hepes (pH 7.4), 1,8 mg/ml glucose and heat inactivated FBS (1% for microscopy experiments, otherwise 5%).

Plasmid constructs

The human $p47^{phox}$ gene (kind gift from Marie-Claire Dagher, Grenoble, France) was amplified by PCR by using primers designed to discard the stop codon of this gene and to introduce HindIII and AgeI restriction sites. By using the Quickchange II Site Directed Mutagenesis kit (Agilent technologies, Santa Clara, CA), the start codon of the pEGFP-N1 vector (Clontech, Palo Alto, CA) was deleted in order to avoid expression of the GFP alone. The p47-GFP vector was then constructed by cloning the $p47^{phox}$ fragment into the mutated pEGFP-N1 plasmid. The cDNA encoding human Rac2 was amplified from pGEX2T-Rac2 (gift from Marie-Claire Dagher, Grenoble, France) by PCR and the PCR fragment was then cloned in the pECFP-C1 vector using the restriction sites HindIII-SacII. The GFP-Rac2G12V and GFP-Rac1G12V vectors were obtained by cloning Rac2G12V or Rac1G12V into the pEGFP-C1 vector (Clontech). The human lactadherin C2 domain (475bp) was amplified by PCR from a vector pBluescript II KS+BA46 (kind gift from C. Théry, Paris, France). The primers used contained restriction sites (Hind III and Sac II) to allow the cloning into the pECFP-C1 vector (Clontech). MCherry was amplified from p413GPDmCherry (kind gift from R. Tsapis, Paris, France) by PCR and the pmCherryC1 vector was obtained by replacing EGFP in the pEGFP-C1 vector by mCherry, using the restriction site AgeI-HindII. The mCherry-lactC2 vector was constructed by inserting the lactC2

domain from pECFP-C1lactC2 into the pmCherryC1 vector at the restriction site Hind III, Sac II. All constructs were controlled by sequencing.

Transient and stable transfection

Differentiated PLB-985 cells were transiently transfected using the Nucleofector device or the 4D-Nucleofector (Lonza, Basel, Switzerland) according to the manufacturer's protocol. For each condition, using the Nucleofector kit for human dendritic cells and the U-015 program or the SF Cell Line Kit and the EH-100 program, 2.10^6 cells were nucleofected with 1 to 4 µg of vector and incubated in culture medium without antibiotics. Four hours post-transfection, cells were processed for experiments. CFP-Rac2 and p47-GFP expressing PLB-985 cell lines were generated as previously described (Tlili et al., 2012). These cell lines were cultured continuously in the presence of 0.5 mg/ml of G418 to maintain the selection.

Preparation and opsonization of yeasts, DCFH2-yeasts and zymosan

Yeasts (*Saccharomyces cerevisiae*) and zymosan particles from *Saccharomyces cerevisiae* (Sigma, Saint Louis, MO) were prepared as described previously (Tlili et al., 2011). To measure the intraphagosomal ROS production, yeasts and zymosan were covalently labeled with 2', 7'-dichlorodihydrofluorescein diacetate, succinimidyl ester (OxyBURST Green H2DCFDA, succinimidyl ester from Life Technologies, Saint Aubin, France) as described (Tlili et al., 2011). Yeasts (10^8 /ml), $DCFH_2$-yeasts were washed and resuspended in PBS (same concentration) before opsonization by incubation with polyclonal rabbit anti-yeast serum (50% diluted, 1 hour, 37°C). Opsonized yeasts were washed twice with PBS, resuspended in Hepes buffer ($5x10^7$/ml). Zymosan or $DCFH_2$-zymosan were opsonized with total human serum following the same protocol as for yeasts and resuspended in Hepes buffer (20 mg/ml).

Cell preparation for microscopy

For some experiments, cells ($2x10^6$ /ml) were loaded with 2 µM of the cytoplasmic cell tracer calcein blue-AM (Life Technologies) during 10 min at room temperature and then washed once. For in vivo imaging, 50 µl of cells ($4x10^6$ /ml in saline media) were allowed to adhere on glass coverslips for 5 min at 37°C and 450 µl of warm Hepes buffer were added.

Live cell imaging

The localization of the mCherry-lactC2 probe was assessed at 37°C by using a DM IRE2 microscope (Leica, Nanterres, France) with a 100x plan Apo 1.4 oil immersion objective, a stage incubator and a Cool SNAP HQ2 camera (Photometrics, Huntington Beach, CA) driven by the Metamorph 7 software (Universal imaging,Westchester, PA). Stacks of 9 frames with a z-optical spacing of 1 µm were collected every minute for 20 min. Images were deconvoluted with Metamorph 7 software and single z planes were extracted. To monitor the intraphagosomal ROS production and p47-GFP phagosomal recruitment in cells co-expressing or not mCherry-lactC2, images were acquired by using a wide field fluorescence microscope described elsewhere (Tlili et al., 2011). Serial images were recorded every 5 s for about 20 min, except for the DCF fluorescence which was recorded every 2 s with binning 2 for up to 40 min. Phagocytosis of opsonized zymosan by GFP-Rac2G12V or GFP Rac1G12V cells cotransfected or not with mCherry-lactC2, was filmed at 37°C by using a spinning disk confocal system (Yokogawa CSU-X1-A1, Yokogawa Electrics, Japan) mounted on a Nikon Eclipse Ti E inverted microscope equipped with a 100x plan Apo 1,4 oil immersion objective and an EM-CCD eVolve camera

(Photometrics) driven by the Metamorph 7 software (Universal imaging). The temperature was maintained at 37°C using a stage incubator. GFP and mCherry were excited at 491 nm and 561 nm respectively by using a laser illumination for 0.3 and 0.2 s and the fluorescence was detected with a quad band beamsplitter, a 525 nm emission filter for GFP and a 607 nm emission filter for mCherry. Sequential stacks of images were collected for several minutes with a time lapse of 10 s or 30s and an optical spacing of 1 µm.

Fluorescence quantification: intraphagosomal ROS production and recruitment of $p47^{phox}$ and Rac2G12V

All images were analyzed with the ImageJ software. To measure DCF fluorescence, ROIs that cover the whole yeast were manually drawn and the mean fluorescence intensity of these ROIs was calculated for each time point. The accumulation of lactC2 at the phagosomal membrane was measured by calculating a fluorescence ratio between the mean fluorescence intensity of the phagosomal ring and the mean cytoplasmic fluorescence intensity. The fluorescence intensity of non phagocyting cells remained stable indicating that there was no photobleaching during the experiments. To quantify p47-GFP fluorescence without artifacts due to volume variations when using wide field microscopy, ratiometric films were obtained with the cytosolic marker calcein blue. The ratio between the GFP and the calcein blue fluorescence was determined after background subtraction. These ratiometric films were then used to analyze $p47^{phox}$ translocation to the phagosome. P47–GFP, GFP-Rac2G12V or GFP-Rac1G12V phagosomal membrane recruitment were determined by evaluating the accumulation of the fusion proteins at the phagosomal membrane relative to the cytoplasm, as described above for the lactC2 probe. A fluorescence ratio higher than 1 indicates that the protein is accumulated at the phagosomal membrane.

Immunofluorescence

The immunofluorescence experiments were performed as described before (Tlili et al., 2012). Briefly, the cells were mixed with opzonised Texas Red zymosan, spun down at 13°C to synchronize phagocytosis and then incubated at 37°C for 0 to 10 min. The cells were fixed with 4% paraformaldehyde, permeabilized with 0,1% tritonX100 in PBS and blocked with 10% decomplemented human serum for 1h at 37°C. The cells were then immunostained with anti-$p47^{phox}$ antibody (BD Bioscience, diluted 1:100) followed by Alexa 488 goat anti-mouse (Life Technologies). Cells were imaged on a spinning disk microscope described above.

Subcellular fractionation, immunoprecipitation and western blotting

To analyze the expression of the fusion protein in the stable p47-GFP or CFP-Rac2 expressing cell line, cells were disrupted in lysis buffer (40000 cells/µl) containing Hepes-Na 25 mM, NaCl 150 mM, $MgCl_2$ 5 mM, EGTA 0.5 mM, TritonX100 0.5%, NaF 10 mM and supplemented with a protease inhibitor cocktail (Roche, Basel, Switzerland). Protein concentration was determined using the BioRad Protein assay (BioRad) and 25 µg of the samples were diluted in 6x Laemmli buffer and boiled for 5 min. The proteins were separated on a 12% SDS-PAGE gel and transferred onto nitrocellulose membrane (BioRad, Marnes La Coquette, France). The membranes were blotted with anti-GFP monoclonal antibody (Roche, diluted 1:500) or anti-$p47^{phox}$ monoclonal antibody (BD Bioscience, diluted 1:1000) or anti-Rac2 rabbit polyclonal antibody (diluted 1:1000, Millipore) followed by incubation with horseradish peroxidase conjugated secondary antibodies (GE Healthcare). Proteins were detected by using the ECL reagent (GE Healthcare Europe, Orsay, France) and the image acquisition system Fusion Fx7

(Fisher Scientific, Illkirch, France). Relative protein quantification on western blot was done using BioD1 software (Fisher Scientific).
Subcellular fractionation was adapted from Dang et al. (Dang et al., 1999). The two differentiated cells lines CFP-Rac2 and p47-GFP were incubated at 37°C first with 5 µM of cytochalasinB for 10 min and then stimulated with 200 nM PMA for 10 min. The stimulation was stopped on ice by addition of ice cold PBS and cells were resuspended in relaxation buffer (100 mM KCl, 3 mM NaCl, 3.5 mM $MgCl_2$, 10 mM Pipes KOH pH7.3, and 1mM EGTA) supplemented with protease inhibitors and NaF(10mM). Cells were disrupted by sonication for 3 x 10 s on ice, and the unbroken cells and nuclei were removed by a 400 g centrifugation for 8 min. The supernatants were transferred to a sucrose gradient (16%-32%) and ultracentrifuged at 200000 g for 30 min (Centrikon T-2050, Kontron Medical, S^t Germain en Laye, France). The plasma membrane fraction was collected and ultracentrifuged at 200000g for 30 min. The membrane pellet was resuspended in relaxation buffer with 1% triton and incubated 30 min at 4°C to solubilize the proteins. Then 5 µg of mouse monoclonal anti- $gp91^{phox}$ (Abcam, Cambrige, UK) were added and the mixture was incubated at 4°C for 1 h. For negative controls, antibodies were omitted. Protein G-agarose beads were added and the mixture was again incubated for 1 h at 4°C. The beads were collected, washed with relaxation buffer with 1% triton, then resuspended in 50 µl of 2x Laemmli sample buffer, boiled and centrifuged at 14 000 g for 5 min. The supernatants were subjected to SDS-PAGE followed by immunoblotting with anti-$gp91^{phox}$ (diluted 1:1000), anti-$p47^{phox}$, anti-GFP, anti-$p67^{phox}$ (Millipore, Bedford, MA) and anti-Rac2.

Statistical analysis and mathematical models

All data are presented as mean ± SEM. Statistical analysis of the quantification of the LactC2 probe at the phagosomal membrane was performed using a Mann Whitney test with GraphPad Prism 5 software. Values of $p < 0.05$ were considered statistically significant.
The ROS production kinetics over 30 min measured by videomicroscopy was analyzed using nonlinear mixed effects models. We assumed that the production of ROS by NADPH oxidase corresponds to an enzymatic kinetics. Thus we have tested several sigmoid models to describe the ROS production and selected the function:
$F(t) = Fmin + (Fmax-Fmin)/(1+e^{-\alpha(t-Tc)})$, where F(t) is the fluorescence at time t, Fmin is the fluorescence base line, Fmax is the maximal fluorescence, Tc is the time when 50% of the maximal fluorescence increase is reached, and α is proportional to the slope of the tangent at Tc. A lactC2 effect was assumed to occur on parameters α and Tc, and this effect was modelled as $\alpha_{lactC2} = \alpha_{control} \exp(\beta_\alpha)$, and $Tc_{lactC2} = Tc_{control} \exp(\beta_{Tc})$.
Statistical analysis was performed using the Monolix software (http://www.monolix.org/, user guide) that is mainly dedicated to pharmacokinetics-pharmacodynamics applications in a population approach. The parameters of the structural model (i.e. Fmin, Fmax, α and Tc) are assumed to be random variables in the population. We assumed that Fmin is constant in each condition, and Fmax, α and Tc are random variables that have a log-normal distribution. The Wald nullity test was used to test if $\beta\alpha=0$ or $\beta Tc=0$, i.e. to compare the logTc and logα values in the two conditions and to statistically determine whether the kinetics of the two cell populations is different or not. Here, p-values < 0.05 indicate that the observed differences for Tc were statistically significantThen we have simulated data (N=100000) and calculated the two simulated cell population parameters that are representative of experimental data, by using Monte-Carlo methods. In order to illustrate the statistical difference observed between the two cell populations, the initial reaction rate at the time of phagosome closure was calculated in each cell population by deriving the function F(t) at time 0 min.

To analyze the effect of the lactC2 probe on $p47^{phox}$ phagosomal recruitment, the same strategy described above was applied. The statistical model used to describe $p47^{phox}$ recruitment derives from a monocompartmental pharmacokinetics model:
$R(t) = R_{inf} + A*e^{(-k_1 t)} – (R_{inf} + A – R_0)*e^{(-k_2 t)}$, where R_{inf} is the fluorescence ratio base line, A is a factor that determines the amplitudes of the two exponentials, R_0 is the ratio at time of phagosome closure, k_1 is a constant of detachment of $p47^{phox}$ and k_2 is a constant of its recruitment. We assumed that a lactC2 effect occurred on parameters k_1 and k_2. The parameters R_{inf}, A, R_0, k_1 and k_2 are random variables that have a log-normal distribution. By using the Monolix software, the parameters were estimated. Data simulation was performed by Monte Carlo method to calculate the time when maximal fluorescence ratio (R_{max}) was reached (T_{max}). This time can be defined as the point when the derivative of the function is null.

Author contribution

M.C.F., J.C.S. and S.D-C. designed, performed and analyzed the experiments. M.D. and M.L. are professional statisticians who modelized the data. M.P. and M-H.C.contributed to imaging experiments. C.M. contributed to the molecular biology experiments. E.T. and O.N. participated in designing the study and writing the paper. S.D-C. designed the study and wrote the paper.

Funding

This work was supported by grants from the French research ministry, programs ACI DRAB and Microbiology, the French League against cancer and the BQR-program of University Paris-Sud.

Acknowledgement

cDNA for the human $p47^{phox}$ gene and for the human lactadherin C2 domain were kind gifts from Marie-Claire Dagher, Grenoble, France and C. Théry, Paris, France. MCF was a recipient of an AFR PhD Grant from the Fonds National de la Recherche – Luxembourg. We wish to thank Sebastien Plançon for help. This work has benefited from the facilities and expertise of IMAGIF (Centre de recherche de Gif); we thank Marie Noelle Soler for her help on the spinning disk confocal. We also thank Marie Erard for her help and her critical reading of the manuscript.

References

Ago, T., Kuribayashi, F., Hiroaki, H., Takeya, R., Ito, T., Kohda, D. and Sumimoto, H. (2003). Phosphorylation of p47phox directs phox homology domain from SH3 domain toward phosphoinositides, leading to phagocyte NADPH oxidase activation. Proc Natl Acad Sci U S A 100, 4474-9.

Allen, L. A., DeLeo, F. R., Gallois, A., Toyoshima, S., Suzuki, K. and Nauseef, W. M. (1999). Transient association of the nicotinamide adenine dinucleotide phosphate oxidase subunits p47phox and p67phox with phagosomes in neutrophils from patients with X-linked chronic granulomatous disease. Blood 93, 3521-30.

Ambruso, D. R., Knall, C., Abell, A. N., Panepinto, J., Kurkchubasche, A., Thurman, G., Gonzalez-Aller, C., Hiester, A., deBoer, M., Harbeck, R. J. et al. (2000). Human neutrophil

immunodeficiency syndrome is associated with an inhibitory Rac2 mutation. Proc Natl Acad Sci U S A 97, 4654-9.

Andersen, M. H., Graversen, H., Fedosov, S. N., Petersen, T. E. and Rasmussen, J. T. (2000). Functional analyses of two cellular binding domains of bovine lactadherin. Biochemistry 39, 6200-6.

Asano, K., Miwa, M., Miwa, K., Hanayama, R., Nagase, H., Nagata, S. and Tanaka, M. (2004). Masking of phosphatidylserine inhibits apoptotic cell engulfment and induces autoantibody production in mice. J Exp Med 200, 459-67.

Botelho, R. J., Teruel, M., Dierckman, R., Anderson, R., Wells, A., York, J. D., Meyer, T. and Grinstein, S. (2000). Localized biphasic changes in phosphatidylinositol-4,5-bisphosphate at sites of phagocytosis. J Cell Biol 151, 1353-68.

Caron, E. and Hall, A. (1998). Identification of two distinct mechanisms of phagocytosis controlled by different Rho GTPases. Science 282, 1717-21.

Conesa-Zamora, P., Lopez-Andreo, M. J., Gomez-Fernandez, J. C. and Corbalan-Garcia, S. (2001). Identification of the phosphatidylserine binding site in the C2 domain that is important for PKC alpha activation and in vivo cell localization. Biochemistry 40, 13898-905.

Dang, P. M., Dewas, C., Gaudry, M., Fay, M., Pedruzzi, E., Gougerot-Pocidalo, M. A. and El Benna, J. (1999). Priming of human neutrophil respiratory burst by granulocyte/macrophage colony-stimulating factor (GM-CSF) involves partial phosphorylation of p47(phox). J Biol Chem 274, 20704-8.

Filippi, M. D., Harris, C. E., Meller, J., Gu, Y., Zheng, Y. and Williams, D. A. (2004). Localization of Rac2 via the C terminus and aspartic acid 150 specifies superoxide generation, actin polarity and chemotaxis in neutrophils. Nat Immunol 5, 744-51.

Finkielstein, C. V., Overduin, M. and Capelluto, D. G. (2006). Cell migration and signaling specificity is determined by the phosphatidylserine recognition motif of Rac1. J Biol Chem 281, 27317-26.

Groemping, Y. and Rittinger, K. (2005). Activation and assembly of the NADPH oxidase: a structural perspective. Biochem J 386, 401-16.

Hanayama, R., Tanaka, M., Miwa, K., Shinohara, A., Iwamatsu, A. and Nagata, S. (2002). Identification of a factor that links apoptotic cells to phagocytes. Nature 417, 182-7.

Hoppe, A. D. and Swanson, J. A. (2004). Cdc42, Rac1, and Rac2 display distinct patterns of activation during phagocytosis. Mol Biol Cell 15, 3509-19.

Johnson, J. L., Ellis, B. A., Munafo, D. B., Brzezinska, A. A. and Catz, S. D. (2006). Gene transfer and expression in human neutrophils. The phox homology domain of p47phox translocates to the plasma membrane but not to the membrane of mature phagosomes. BMC Immunol 7, 28.

Kanai, F., Liu, H., Field, S. J., Akbary, H., Matsuo, T., Brown, G. E., Cantley, L. C. and Yaffe, M. B. (2001). The PX domains of p47phox and p40phox bind to lipid products of PI(3)K. Nat Cell Biol 3, 675-8.

Karathanassis, D., Stahelin, R. V., Bravo, J., Perisic, O., Pacold, C. M., Cho, W. and Williams, R. L. (2002). Binding of the PX domain of p47(phox) to phosphatidylinositol 3,4-bisphosphate and phosphatidic acid is masked by an intramolecular interaction. EMBO J 21, 5057-68.

Kay, J. G., Koivusalo, M., Ma, X., Wohland, T. and Grinstein, S. (2012). Phosphatidylserine dynamics in cellular membranes. Mol Biol Cell 23, 2198-212.

Lavielle, M. and Mentre, F. (2007). Estimation of population pharmacokinetic parameters of saquinavir in HIV patients with the MONOLIX software. J Pharmacokinet Pharmacodyn 34, 229-49.

Li, X. J., Marchal, C. C., Stull, N. D., Stahelin, R. V. and Dinauer, M. C. (2010). p47phox Phox homology domain regulates plasma membrane but not phagosome neutrophil NADPH oxidase activation. J Biol Chem 285, 35169-79.

Magalhaes, M. A. and Glogauer, M. (2010). Pivotal Advance: Phospholipids determine net membrane surface charge resulting in differential localization of active Rac1 and Rac2. J Leukoc Biol 87, 545-55.

McLaughlin, S. and Aderem, A. (1995). The myristoyl-electrostatic switch: a modulator of reversible protein-membrane interactions. Trends Biochem Sci 20, 272-6.

Minakami, R., Maehara, Y., Kamakura, S., Kumano, O., Miyano, K. and Sumimoto, H. (2010). Membrane phospholipid metabolism during phagocytosis in human neutrophils. Genes Cells 15, 409-24.

Mizrahi, A., Berdichevsky, Y., Casey, P. J. and Pick, E. (2010). A prenylated p47phox-p67phox-Rac1 chimera is a Quintessential NADPH oxidase activator: membrane association and functional capacity. J Biol Chem 285, 25485-99.

Nauseef, W. M. (2004). Assembly of the phagocyte NADPH oxidase. Histochem Cell Biol 122, 277-91.

Quinn, M. T., DeLeo, F. R. and Bokoch, G. M. (2007). Neutrophil methods and protocols. Preface. Methods Mol Biol 412, vii-viii.

Quinn, M. T., Evans, T., Loetterle, L. R., Jesaitis, A. J. and Bokoch, G. M. (1993). Translocation of Rac correlates with NADPH oxidase activation. Evidence for equimolar translocation of oxidase components. J Biol Chem 268, 20983-7.

Roy, M. O., Leventis, R. and Silvius, J. R. (2000). Mutational and biochemical analysis of plasma membrane targeting mediated by the farnesylated, polybasic carboxy terminus of K-ras4B. Biochemistry 39, 8298-307.

Shao, C., Novakovic, V. A., Head, J. F., Seaton, B. A. and Gilbert, G. E. (2008). Crystal structure of lactadherin C2 domain at 1.7A resolution with mutational and computational analyses of its membrane-binding motif. J Biol Chem 283, 7230-41.

Shi, J. and Gilbert, G. E. (2003). Lactadherin inhibits enzyme complexes of blood coagulation by competing for phospholipid-binding sites. Blood 101, 2628-36.

Shi, J., Heegaard, C. W., Rasmussen, J. T. and Gilbert, G. E. (2004). Lactadherin binds selectively to membranes containing phosphatidyl-L-serine and increased curvature. Biochim Biophys Acta 1667, 82-90.

Shpungin, S., Dotan, I., Abo, A. and Pick, E. (1989). Activation of the superoxide forming NADPH oxidase in a cell-free system by sodium dodecyl sulfate. Absolute lipid dependence of the solubilized enzyme. J Biol Chem 264, 9195-203.

Stahelin, R. V., Burian, A., Bruzik, K. S., Murray, D. and Cho, W. (2003). Membrane binding mechanisms of the PX domains of NADPH oxidase p40phox and p47phox. J Biol Chem 278, 14469-79.

Stasia, M. J. and Li, X. J. (2008). Genetics and immunopathology of chronic granulomatous disease. Semin Immunopathol 30, 209-35.

Steinberg, B. E. and Grinstein, S. (2008). Pathogen destruction versus intracellular survival: the role of lipids as phagosomal fate determinants. J Clin Invest 118, 2002-11.

Tamura, M., Tamura, T., Tyagi, S. R. and Lambeth, J. D. (1988). The superoxide-generating respiratory burst oxidase of human neutrophil plasma membrane. Phosphatidylserine as an effector of the activated enzyme. J Biol Chem 263, 17621-6.

Tlili, A., Dupre-Crochet, S., Erard, M. and Nüsse, O. (2011). Kinetic analysis of phagosomal production of reactive oxygen species. Free Radic Biol Med 50, 438-47.

Tlili, A., Erard, M., Faure, M. C., Baudin, X., Piolot, T., Dupre-Crochet, S. and Nusse, O. (2012). Stable accumulation of p67phox at the phagosomal membrane and ROS production within the phagosome. J Leukoc Biol 91, 83-95.

Ueyama, T., Kusakabe, T., Karasawa, S., Kawasaki, T., Shimizu, A., Son, J., Leto, T. L., Miyawaki, A. and Saito, N. (2008). Sequential binding of cytosolic Phox complex to phagosomes through regulated adaptor proteins: evaluation using the novel monomeric Kusabira-Green System and live imaging of phagocytosis. J Immunol 181, 629-40.

Ugolev, Y., Molshanski-Mor, S., Weinbaum, C. and Pick, E. (2006). Liposomes comprising anionic but not neutral phospholipids cause dissociation of Rac(1 or 2) x RhoGDI complexes and support amphiphile-independent NADPH oxidase activation by such complexes. J Biol Chem 281, 19204-19.

Williams, C. L. (2003). The polybasic region of Ras and Rho family small GTPases: a regulator of protein interactions and membrane association and a site of nuclear localization signal sequences. Cell Signal 15, 1071-80.

Williams, D. A., Tao, W., Yang, F., Kim, C., Gu, Y., Mansfield, P., Levine, J. E., Petryniak, B., Derrow, C. W., Harris, C. et al. (2000). Dominant negative mutation of the hematopoietic-specific Rho GTPase, Rac2, is associated with a human phagocyte immunodeficiency. Blood 96, 1646-54.

Xu, X., Barry, D. C., Settleman, J., Schwartz, M. A. and Bokoch, G. M. (1994). Differing structural requirements for GTPase-activating protein responsiveness and NADPH oxidase activation by Rac. J Biol Chem 269, 23569-74.

Xu, X., Wang, Y., Barry, D. C., Chanock, S. J. and Bokoch, G. M. (1997). Guanine nucleotide binding properties of Rac2 mutant proteins and analysis of the responsiveness to guanine nucleotide dissociation stimulator. Biochemistry 36, 626-32.

Yeung, T., Gilbert, G. E., Shi, J., Silvius, J., Kapus, A. and Grinstein, S. (2008). Membrane phosphatidylserine regulates surface charge and protein localization. Science 319, 210-3.

Yeung, T. and Grinstein, S. (2007). Lipid signaling and the modulation of surface charge during phagocytosis. Immunol Rev 219, 17-36.

Yeung, T., Heit, B., Dubuisson, J. F., Fairn, G. D., Chiu, B., Inman, R., Kapus, A., Swanson, M. and Grinstein, S. (2009). Contribution of phosphatidylserine to membrane surface charge and protein targeting during phagosome maturation. J Cell Biol 185, 917-28.

Yeung, T., Terebiznik, M., Yu, L., Silvius, J., Abidi, W. M., Philips, M., Levine, T., Kapus, A. and Grinstein, S. (2006). Receptor activation alters inner surface potential during phagocytosis. Science 313, 347-51.

Figure legends

Figure 1 Generation of stable PLB-985 cell lines expressing p47-GFP and CFP-Rac2
(A, B, C) Generation of p47–GFP and CFP-Rac2 expressing stable cell lines: (A) Western blot analysis of p47-GFP (left panel) and CFP-Rac2 (right panel) using an anti-GFP antibody. (B) Western blot analysis of p47–GFP using an anti-$p47^{phox}$ antibody. (C) Western blot analysis of CFP-Rac2 using an anti-Rac2 antibody. (D, E): Differentiated PLB-985 cells expressing p47-GFP (D) or CFP-Rac2 (E) were stimulated for 10 min with PMA and then lysed by sonication. Membrane and cytosol were separated by ultracentrifugation on sucrose gradient. Membrane fractions were immunoprecipitated (IP) with antibodies specific for $gp91^{phox}$. The negative control contained no antibody during precipitation. Immunoprecipitates were resolved by SDS-PAGE followed by immunoblotting with anti-$gp91^{phox}$, anti-$p47^{phox}$, anti-Rac2, anti-GFP and anti-$p67^{phox}$ antibodies. The star marks the heavy chain of Immunoglobulin G anti-$gp91^{phox}$

Figure 2. Recruitment of p47 during phagocytosis of opsonized zymosan
(A, B, C) Wide-field videomicroscopy was used to monitor phagocytosis of zymosan (*) by p47-GFP expressing cells. (A) Representative micrographs of ratiometric films between p47-GFP and the cytosolic marker calcein blue. Scale bar, 5 µm. (B) The time of the first appearance of p47-GFP on the phagosome membrane was analyzed for 13 positive phagosomes. The time of phagosome closure is defined as time zero. The mean is represented by a black line. (C) P47-GFP accumulation at the phagosomal membrane was quantified by calculating the relative fluorescence intensity at the phagosomal membrane compared to the cytosol on the ratiometric films. At least ten phagosomes per condition were analyzed and are shown as mean ± SEM. Time 0 (black arrow) corresponds to the phagosome closure.
(D, E) Immunofluorescence experiments were performed to detect endogenous $p47^{phox}$-positive phagosomes at 0, 2, 5 and 10 min after incubation of the cells with texas red opsonized zymosan at 37°C. (D) Representative micrographs at time 2 and 10 min are shown. The phagosomes are indicated by arrows. The arrow in the left micrograph shows a $p47^{phox}$-positive phagosome. (E, left panel) Percentage of phagosomes ((number of phagosomes/number of cells)*100) at the different time points. For each condition, in each experiment, at least 150 cells have been observed. (E, right panel) Percentage of $p47^{phox}$-positive phagosomes at the different time points. The results represent the mean of at least three independent experiments.

Figure 3. Recruitment of GFP-Rac2G12V during phagocytosis of opsonized zymosan
Cells were transiently transfected with GFP-Rac2G12V. (A) Representative micrographs of zymosan (*) phagocytosis by transfected cells acquired by spinning-disk confocal videomicroscopy. Time 0 was set when the phagosome closure was observed. Scale bar, 5 µm. (B) The time of the first appearance of GFP-Rac2G12V on phagosome membrane was analyzed for 11 positive phagosomes. The time of phagosome closure is defined at time zero. The mean is represented by a black line. (C) GFP-Rac2G12V accumulation at the phagosomal membrane was quantified by calculating the relative fluorescence intensity at the phagosomal membrane compared to the cytosol. Data are mean ± SEM from at least seven phagosomes per condition. Time 0 (black arrow) corresponds to the phagosome closure.

Figure 4. Localization of lactC2 decorated phosphatidylserine during phagocytosis.
(A) Differentiated PLB-985 cells were transiently transfected with mCherry-lactC2, and phagocytosis of yeasts (*) by the transfected cells was imaged by wide field videomicroscopy, followed by a 3D-deconvolution analysis. Time 0 was set when the phagosome closure was observed. Scale bar, 5 µm. (B) Quantification of lactC2 accumulation at the phagosomal membrane was evaluated by measuring the phagosomal fluorescence relative to the cytosolic fluorescence. Data are mean ± SEM from at least seven phagosomes for each time point, * $p < 0.05$.

Figure 5. Recruitment of p47-GFP and CFP-Rac2 in the presence of mcherry-lactC2
(A, B) The p47-GFP transgenic cell line was transiently transfected with mCherry-lactC2. Wide-field videomicroscopy was used to monitor phagocytosis of zymosan (*). (A) Representative micrographs of ratiometric films between p47-GFP and the cytosolic marker calcein blue. Scale bar, 5 µm. (B) Quantification of p47 accumulation at the phagosome in the absence (black line) or presence of mcherry-lactC2 (red line). At least ten phagosomes per condition were analyzed and are shown as mean ± SEM. Time 0 (black arrow) corresponds to the phagosome closure.
(C, D) Cells were transfected with GFP-Rac2G12V alone and mCherry-lactC2. (C) Representative micrographs of zymosan (*) phagocytosis by transfected cells were acquired by spinning-disk confocal videomicroscopy. Time 0 was set when the phagosome closure was observed. Scale bar, 5 µm. (C) Quantification of GFP-Rac1G12V at the phagosomal membrane in the absence (black line) or presence of mcherry-lactC2 (red line). Data are mean ± SEM from 8 phagosomes per condition. Time 0 corresponds to the phagosome closure.

Figure 6. Transient accumulation of GFP-Rac1G12V at the phagosome in the absence or presence of mCherry-lactC2
(A, B) Cells were transfected with GFP-Rac1G12V alone (A) or together with mCherry-lactC2 (B). Representative micrographs of zymosan (*) phagocytosis by transfected cells were acquired by spinning-disk confocal videomicroscopy. Time 0 was set when the phagosome closure was observed. Scale bar, 5 µm. (C) Quantification of GFP-Rac1G12V at the phagosomal membrane. Data are mean ± SEM from eight phagosomes per condition. Time 0 corresponds to the phagosome closure.

Figure 7. Effect of lactC2 expression on kinetics of ROS production.
(A) Cells were transfected with mcherry (upper panel) or mcherry-lactC2 (lower panel). Images of phagocytosis by transfected cells at 0 to 10 min after phagosome closure showing mcherry or mcherry-lactC2 (red) and $DCFH_2$ yeast (green). In the lower panel some $DCFH_2$-yeasts outside the mcherry positive cell present a strong fluorescence since they have been phagocytosed by neighboring cells that are negative for mcherry-lactC2. The phagosomes are indicated by an arrow. Time 0 was set when the phagosome closure was observed. Scale bar, 5 µm. (C) The kinetics of the ROS production was assessed by videomicroscopy by quantifying $DCFH_2$-labelled yeast fluorescence in cells with mcherry-lactC2 or mcherry. Time course of the average phagosomal fluorescence (± SEM) during the first 12 min from at least ten $DCFH_2$ labeled yeasts for each time point of both conditions.

Figure 8. Model of NADPH oxidase assembly and phosphatidylserine involvement during phagocytosis
A model for NADPH oxidase activation on the phagosomal membrane based on the literature and the data in this article is shown in 3 steps from left to right: The distribution of NADPH oxidase subunits prior to activation (A), at the beginning of NADPH oxidase activity (B) and during continuous activity beyond 3 to 5 min after phagosome closure (C). The presence of 3 different anionic phospholipids is shown by colored head groups.

Online Supplementary Material

Video S1 : P47-GFP is transiently recruited to the phagosome
Ratiometric film between p47-GFP and the cytosolic marker calcein blue during zymosan (*) uptake. Scale bar 5µm.

Video S2 : GFP-Rac2G12V is transiently recruited to the phagosome
Time lapse video of GFP-Rac2G12V during zymosan (*) uptake. Scale bar 5µm.

Video S3 : GFP-Rac2G12V is no more recruited to the phagosome in the presence of mcherry-lactC2. Time lapse video of GFP-Rac2G12V in the presence of mcherry-lactC2 during phagocytosis of zymosan (*). Scale bar 5µm.

Video S4 : GFP-Rac1G12V starts to detach from the phagosome after sealing
Time lapse video of GFP-Rac1G12V in the presence of mcherry-lactC2 during zymosan (*) uptake. Scale bar 5µm.

Figure S5 : Comparison of the kinetics of the ROS production between the experimental values and the mathematical model
The kinetics of the ROS production was assessed by videomicroscopy by quantifying $DCFH_2$-labelled yeast fluorescence in cells with mcherry-lactC2 or mcherry. Time course of the median of the $DCFH_2$-yeast fluorescence values: the red and pale blue curves represent the median of experimental values, whereas the pink and dark blue curves represent the median of the values predicted by the model.

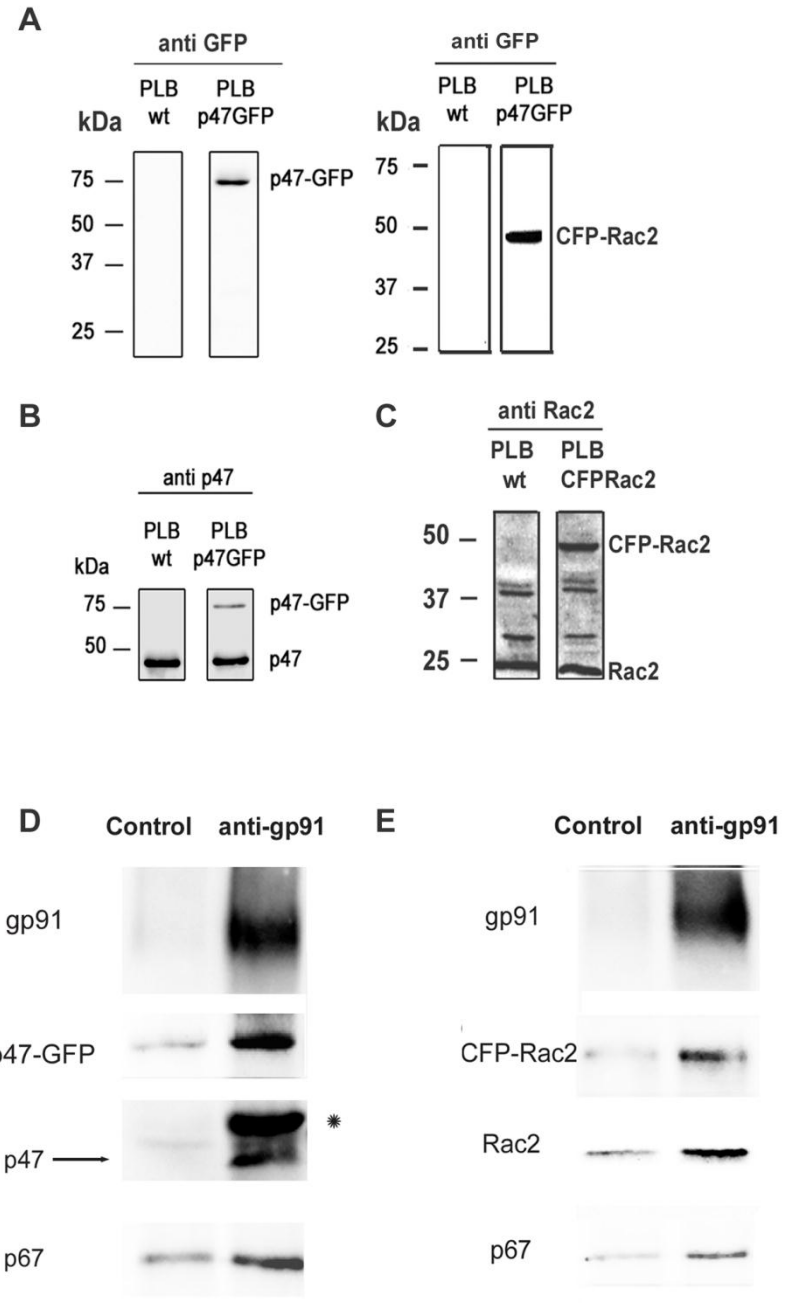
A
anti GFP
PLB wt
PLB p47GFP
kDa
75
50
37
25
p47-GFP
anti GFP
PLB wt
PLB p47GFP
kDa
75
50
37
25
CFP-Rac2
B
anti p47
PLB wt
PLB p47GFP
kDa
75
50
p47-GFP
p47
C
anti Rac2
PLB wt
PLB CFPRac2
50
37
25
CFP-Rac2
Rac2
D
Control
anti-gp91
gp91
p47-GFP
p47
p67
*
E
Control
anti-gp91
gp91
CFP-Rac2
Rac2
p67

Figure 1

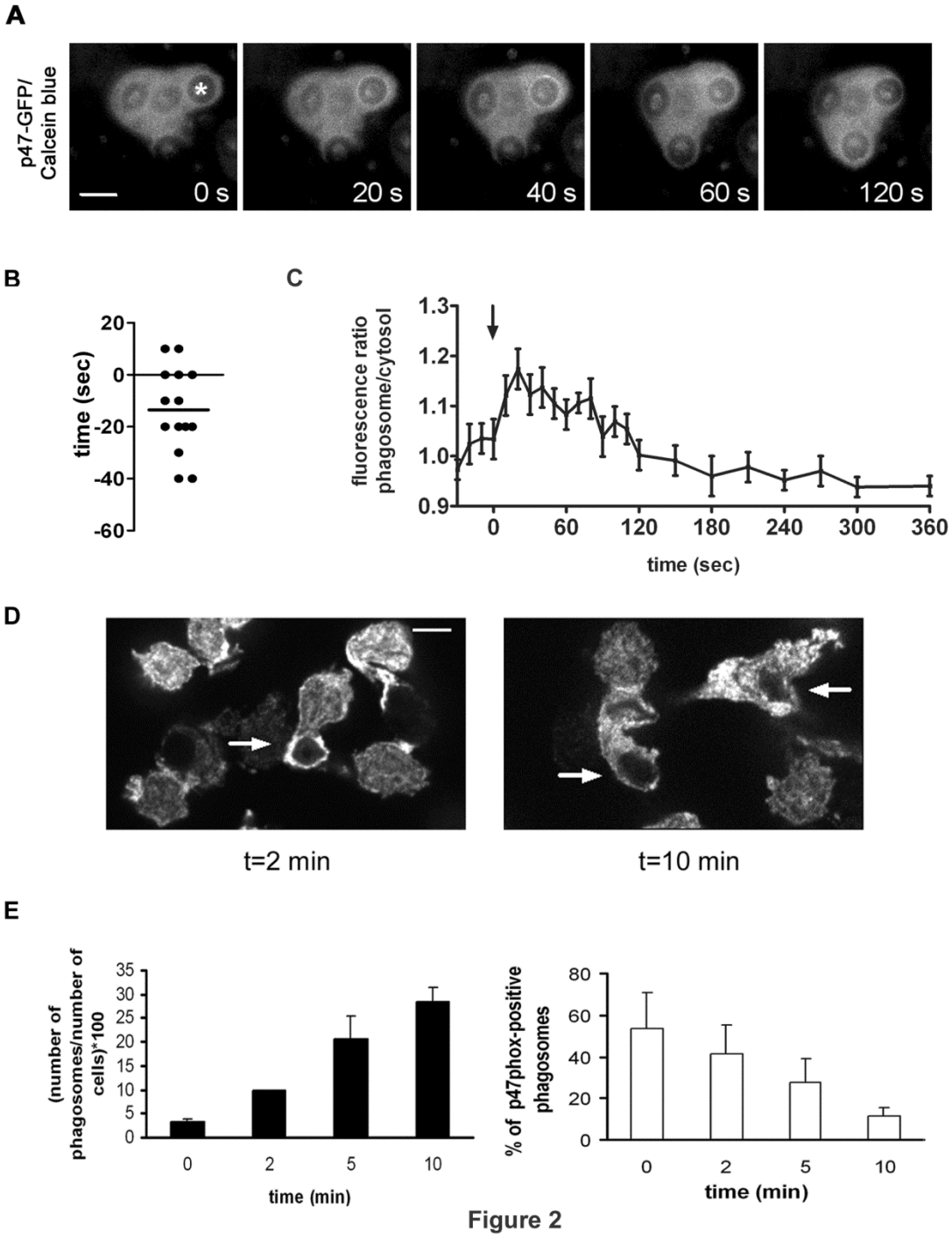
A
p47-GFP/
Calcein blue
0 s
20 s
40 s
60 s
120 s
B
time (sec)
20
0
-20
-40
-60
C
fluorescence ratio
phagosome/cytosol
1.3
1.2
1.1
1.0
0.9
0
60
120
180
240
300
360
time (sec)
D
t=2 min
t=10 min
E
(number of phagosomes/number of cells)*100
35
30
25
20
15
10
5
0
0
2
5
10
time (min)
% of p47phox-positive phagosomes
80
60
40
20
0
0
2
5
10
time (min)

Figure 2

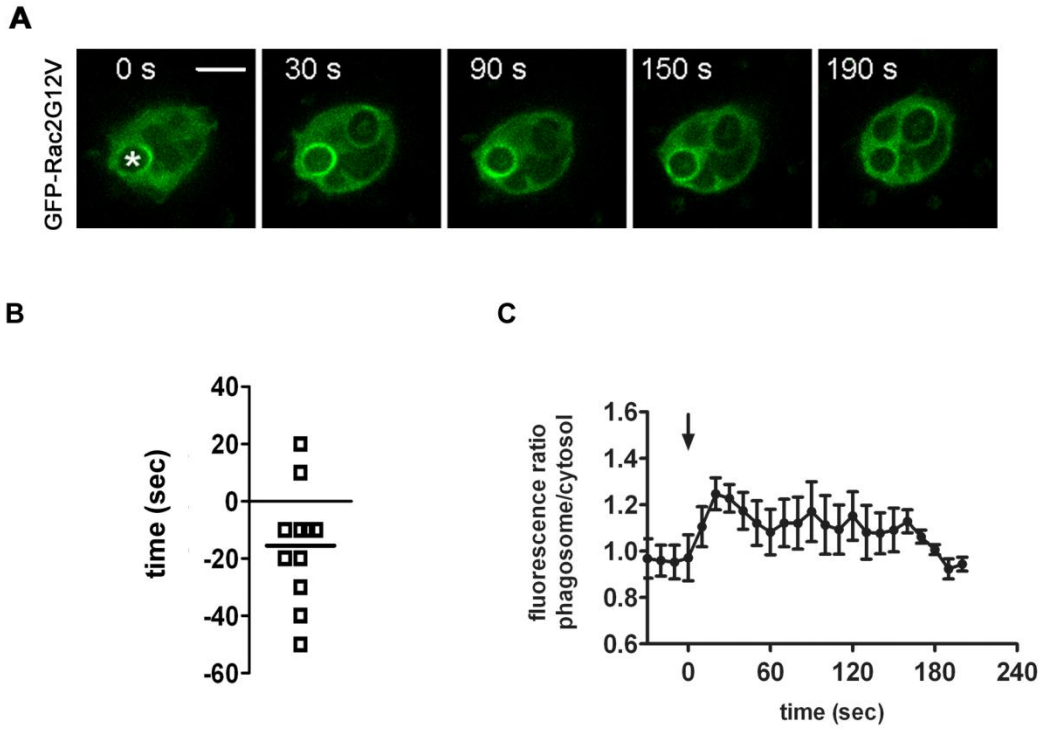
A
GFP-Rac2G12V
0 s
30 s
90 s
150 s
190 s
B
time (sec)
40
20
0
-20
-40
-60
C
fluorescence ratio
phagosome/cytosol
1.6
1.4
1.2
1.0
0.8
0.6
0
60
120
180
240
time (sec)

Figure 3

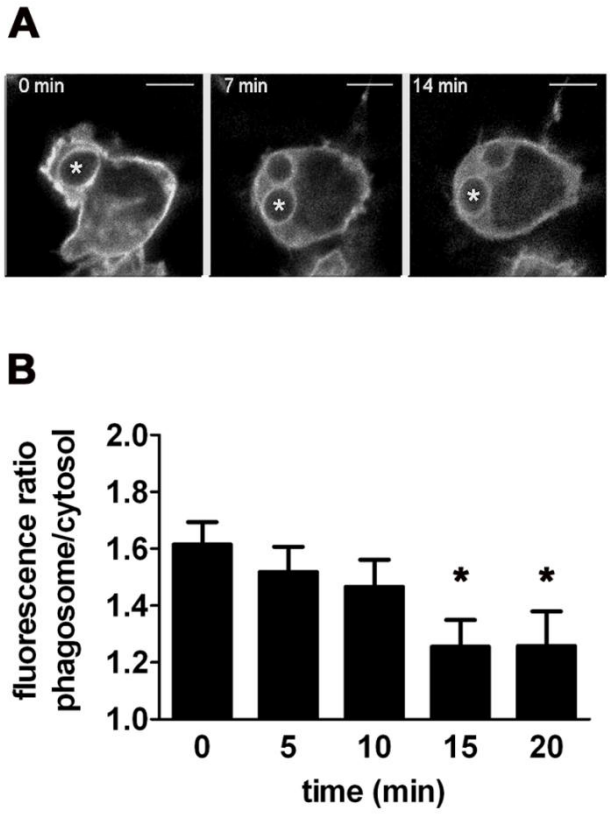
A
0 min
7 min
14 min
B
fluorescence ratio
phagosome/cytosol
2.0
1.8
1.6
1.4
1.2
1.0
0
5
10
15
20
time (min)

Figure 4

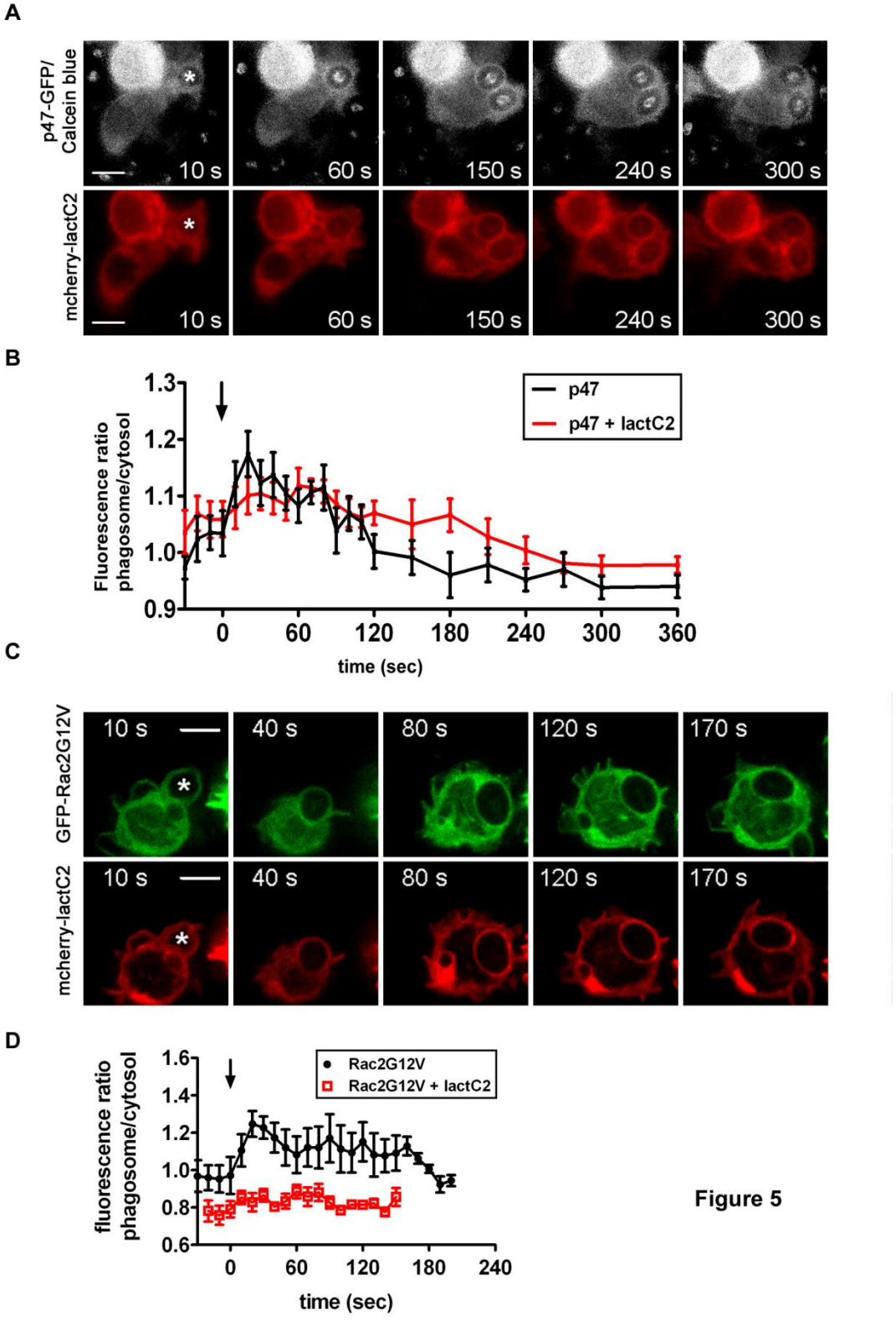
A
p47-GFP/
Calcein blue
10 s
60 s
150 s
240 s
300 s
mcherry-lactC2
10 s
60 s
150 s
240 s
300 s
B
Fluorescence ratio
phagosome/cytosol
1.3
1.2
1.1
1.0
0.9
0
60
120
180
240
300
360
time (sec)
p47
p47 + lactC2
C
GFP-Rac2G12V
10 s
40 s
80 s
120 s
170 s
mcherry-lactC2
10 s
40 s
80 s
120 s
170 s
D
fluorescence ratio
phagosome/cytosol
1.6
1.4
1.2
1.0
0.8
0.6
0
60
120
180
240
time (sec)
Rac2G12V
Rac2G12V + lactC2

Figure 5

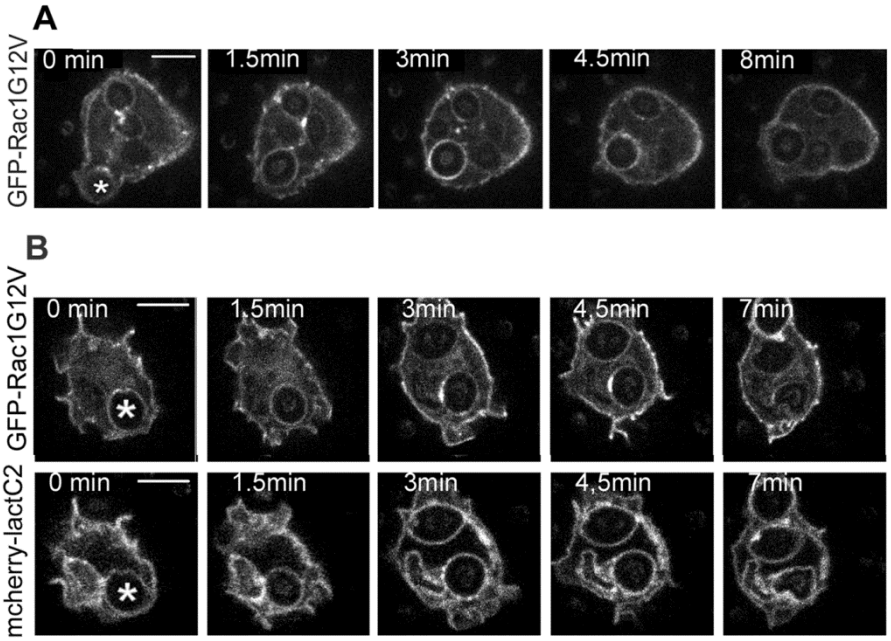
A
GFP-Rac1G12V
0 min
1.5min
3min
4.5min
8min
B
GFP-Rac1G12V
0 min
1.5min
3min
4.5min
7min
mcherry-lactC2
0 min
1.5min
3min
4.5min
7min

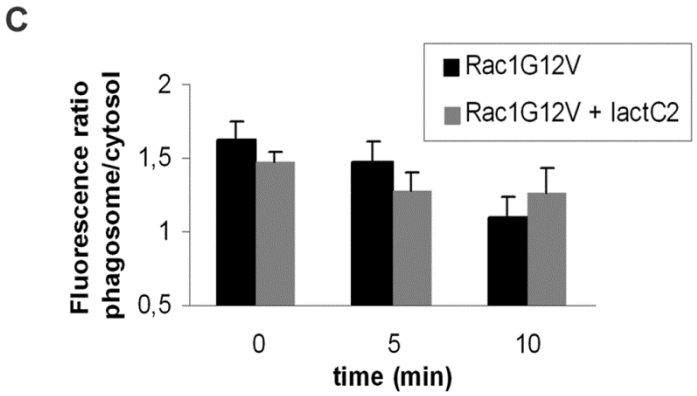
C
Rac1G12V
Rac1G12V + lactC2
Fluorescence ratio phagosome/cytosol
2
1,5
1
0,5
0
5
10
time (min)

Figure 6

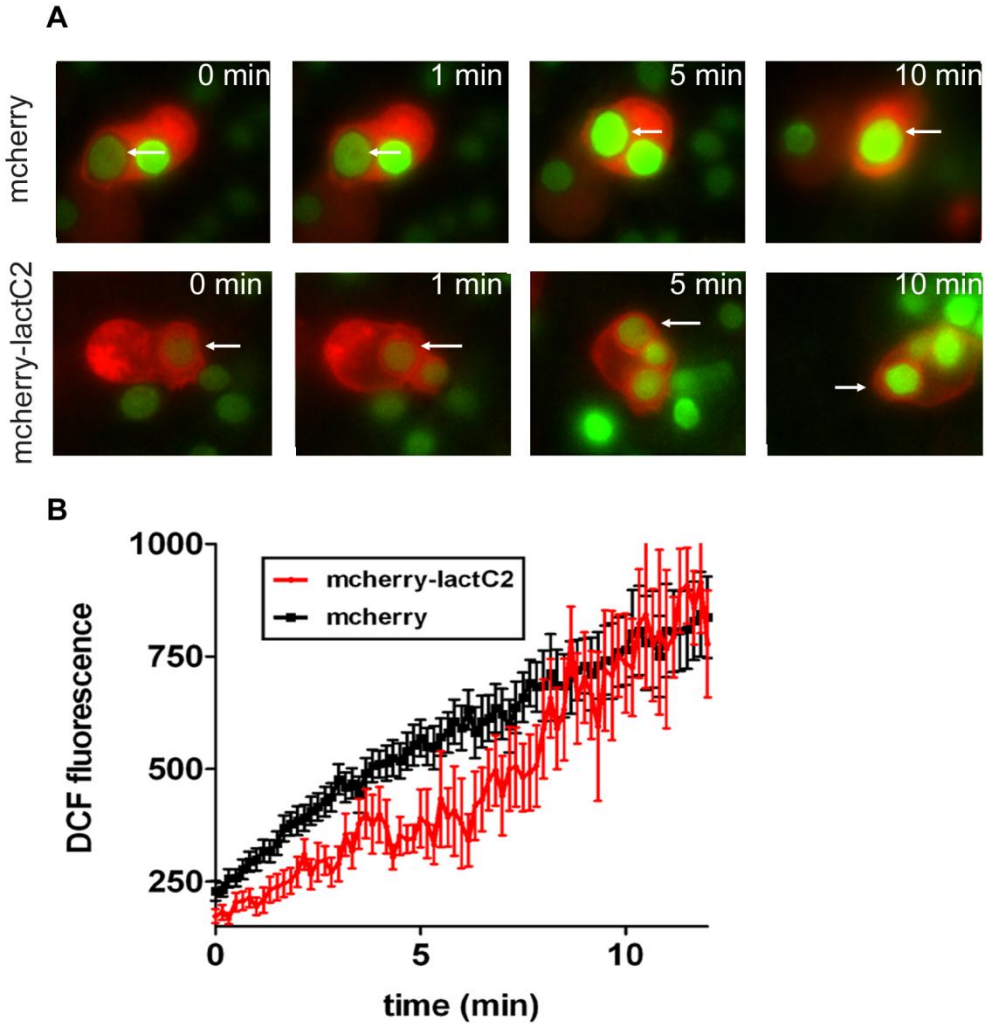
A
mcherry
mcherry-lactC2
0 min
1 min
5 min
10 min
B
DCF fluorescence
1000
750
500
250
0
5
10
time (min)
mcherry-lactC2
mcherry

Figure 7

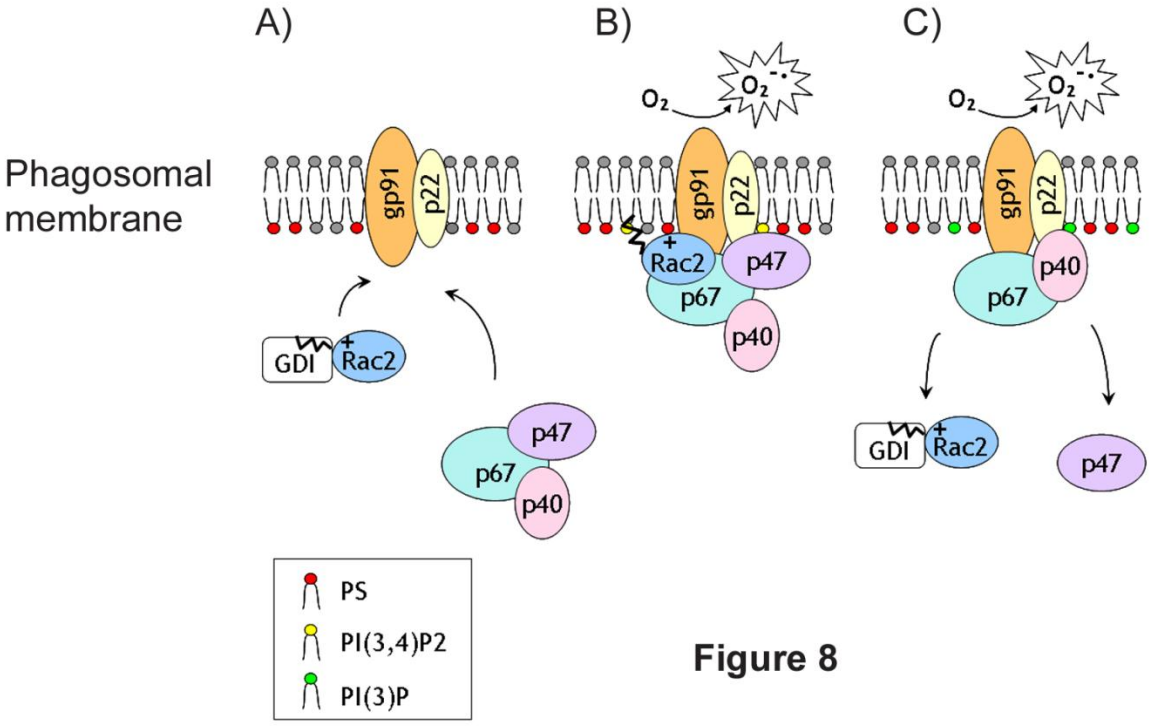
A)
B)
C)
Phagosomal membrane
gp91
p22
GDI
Rac2
p47
p67
p40
O_2
$O_2^{\cdot-}$
PS
PI(3,4)P2
PI(3)P

Figure 8

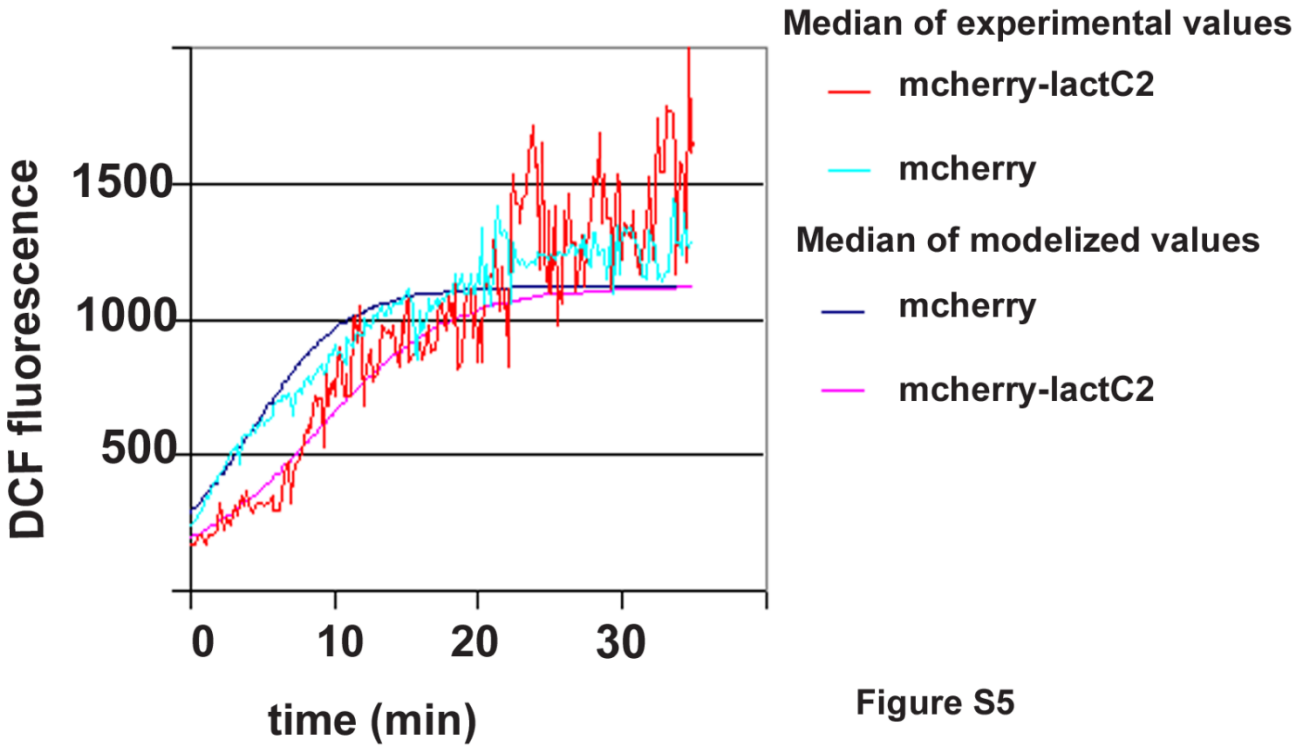
DCF fluorescence
1500
1000
500
0
10
20
30
time (min)
Median of experimental values
mcherry-lactC2
mcherry
Median of modelized values
mcherry
mcherry-lactC2

Figure S5